

Consistent thermal analysis procedure of LNG storage tank

Se-Jin Jeon[†], Byeong-Moo Jin[‡] and Young-Jin Kim^{‡†}

DAEWOO E&C, Institute of Construction Technology, 60 Songjook-dong, Jangan-gu,
Suwon, Kyonggi 440-210, South Korea

Chul-Hun Chung^{‡‡}

Department of Civil and Environmental Engineering, Dankook University, San 8,
Hannam-dong, Youngsan-gu, Seoul 140-714, South Korea

(Received August 22, 2005, Accepted September 19, 2006)

Abstract. As the LNG (Liquefied Natural Gas) tank contains cryogenic liquid, realistic thermal analyses are of a primary importance for a successful design. The structural details of the LNG tank are so complicated that some strategies are necessary to reasonably predict its temperature distribution. The proposed heat transfer model can consider the beneficial effects of insulation layers and a suspended deck on temperature distribution of the outer concrete tank against cryogenic conditions simply by the boundary conditions of the outer tank model. To this aim, the equilibrium condition or heat balance in a steady state is utilized in a various way, and some aspects of heat transfer via conduction, convection and radiation are implemented as necessary. Overall thermal analysis procedures for the LNG tank are revisited to examine some unjustifiable assumptions of conventional analyses. Concrete and insulation properties under cryogenic condition and a reasonable conversion procedure of the temperature-induced nonlinear stress into the section forces are discussed. Numerical examples are presented to verify the proposed schemes in predicting the actual temperature and stress distributions of the tank as affected by the cryogenic LNG for the cases of normal operation and leakage from the inner steel tank. It is expected that the proposed schemes enable a designer to readily detect the effects of insulation layers and a suspended deck and, therefore, can be employed as a useful and consistent tool to evaluate the thermal effect in a design stage of an LNG tank as well as in a detailed analysis.

Keywords: LNG storage tank; cryogenic temperature; heat transfer analysis; thermal stress; leakage; insulations.

1. Introduction

Using natural gas is an effective method for coping with lack of energy resources. Natural gas has

[†] Principal Researcher, Corresponding author, E-mail: jsj@dwconst.co.kr

[‡] Principal Researcher, E-mail: jinbm@dwconst.co.kr

^{‡†} Chief Researcher, E-mail: kimyj@dwconst.co.kr

^{‡‡} Professor, E-mail: chchung5@dankook.ac.kr

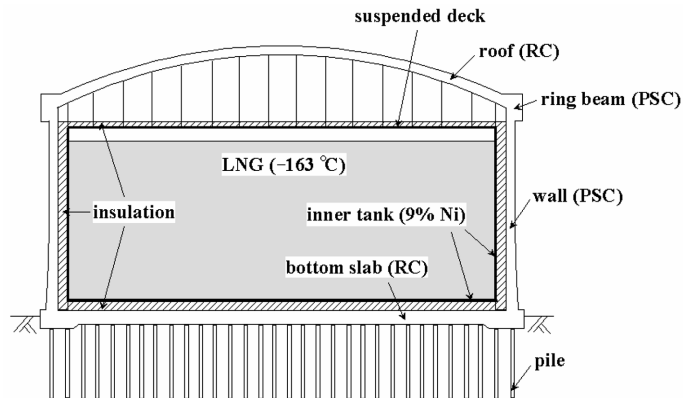


Fig. 1 Full containment above-ground LNG storage tank

found successful applications in city gas, power plants and vehicles. LNG (Liquefied Natural Gas) storage tanks can be effectively used to cope with seasonal fluctuations in natural gas demand. LNG has a cryogenic temperature as low as -163°C to ensure the minimum storage volume when stored in LNG tank. Of the various types of LNG storage tanks, the full containment, above-ground type (Fig. 1) is now employed worldwide; thus, it is selected as the main structural type considered in this study. A typical full containment tank has a double safety system consisting of an outer concrete tank and an inner steel tank. In addition, several types of insulations—in the bottom and wall of the tank, between the outer tank and the inner tank and on the suspended deck—are used to maintain the required boil-off gas rate.

As the LNG tank contains cryogenic liquid, the safety and serviceability (e.g. liquid tightness) of the tank can be ensured only through a reasonable thermal analysis procedure. During normal operation, the inner tank contains LNG (Fig. 1) and the outer tank, by virtue of its insulation system, is not directly exposed to the cryogenic temperature. However, if the LNG leaked from the inner tank, it would soak into the insulation. In the event of such an accident, some insulation layers would be unable to function and the outer concrete tank could be severely affected by a rapid temperature drop. The aforementioned two cases should be considered in a design, but a consistent thermal analysis procedure has not yet been established, as current design documents (DAELIM and DYWIDAG 1995, DAEWOO *et al.* 1999) and recent research (Choi *et al.* 2002) show. The relevant issues can be divided into the following.

- (1) Details of an LNG tank that consists of an inner tank, an outer tank, insulation layers and a suspended deck (Fig. 1) are rather complicated. The proper scope of an analysis model is therefore not easy to establish when the goal is to obtain the temperature and thermal stress distribution of the outer concrete tank. Two alternatives are conceivable: a full or semi-full model containing almost all the components of the tank; and a partial model only considering the outer tank.
- (2) When the partial model is adopted for thermal analysis, the temperature boundary conditions, especially the inner face conditions, of the outer tank should be determined in advance. The effects of the insulation layers and suspended deck on the inner face temperature of the concrete should be carefully and reasonably evaluated. In many cases, however, these effects are overlooked or are evaluated on a basis of unrealistic assumptions.

- (3) According to previous experimental data, some properties of concrete, insulations, reinforcing bars and prestressing tendons change remarkably under cryogenic temperature. Nevertheless, such material changes have often been considered incorrectly or not been considered at all.

Although some recent studies pursue a more refined temperature analysis of the LNG tank (Nakano 2001, Watanabe *et al.* 2003, Chen *et al.* 2004), the availability of a reliable procedure has been quite limited so far due to a lack of the related studies. The purpose of this study is, therefore, to establish a consistent thermal analysis procedure of the full containment type LNG storage tank incorporating cryogenic temperature. To this aim, the partial model is adopted and useful techniques for a heat transfer analysis of the outer concrete tank are proposed in terms of boundary conditions. In addition, the thermal properties of the concrete and insulations under cryogenic temperature condition are taken into account in the analyses if necessary. A scheme for evaluating the section forces from nonlinear distribution of the thermal stresses is proposed. By employing the proposed schemes, a set of numerical examples are presented to clarify the actual temperature and stress distributions of the tank as affected by the cryogenic LNG.

2. General remarks on thermal analysis

As noted, normal operation and leakage conditions are both considered here. LNG can possibly leak from the inner tank in two different ways, depending on the accident scenario: local leakage and overall leakage (Ivanyi 1987). In the local leakage, LNG leaks through a small hole in the inner tank and forms a cold spot on the outer tank. In the overall leakage, LNG continuously leaks until the liquid level becomes constant after filling the space between the outer and inner tanks. Here, the overall leakage problem that makes severer effect on the outer tank is discussed.

One disadvantage of full thermal analysis model that considers all the components inside the LNG tank is that it involves cumbersome and time-consuming tasks in modeling and thus is impractical for design purposes. The proposed method limits the scope of structural modeling to focus on the outer tank while the effects of the multiple insulation layers and the suspended deck on temperature distribution are formulated separately. Therefore, various situations that may occur under typical operation and leakage conditions can be simulated using the same outer tank model by changing the boundary conditions, providing versatility to a designer.

Distribution of the temperature or thermal stresses becomes time-independent after some duration of time when the concrete surface is exposed to temperature change. In other words, it attains a steady state passing through a transient state. Most of the relevant studies and designs have been performed based on the steady state. Likewise, the proposed equations are derived assuming a heat balance condition under this steady state. Once temperature boundary conditions are obtained, heat transfer and thermal stress analyses are performed to yield the temperature distribution and the resulting thermal stresses of the outer tank.

3. Boundary conditions of roof

It is expected that the inner face of the concrete roof is not exposed directly to the cryogenic atmosphere due to the thermal barrier effect of the suspended deck and the deck insulation. Therefore, a suitable methodology needs to be established in order to predict the inner face temperature of the

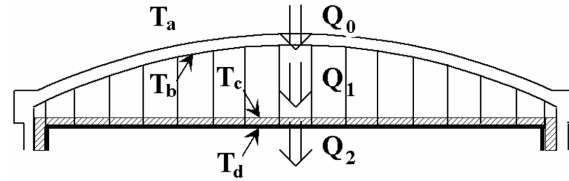


Fig. 2 Heat flow rates through the roof (alternative 1)

roof. Whether LNG leaks or not does not significantly affect the temperature of the roof.

3.1 Alternative 1

Alternative 1 assumes the equilibrium of the heat flow rates penetrating the roof (Fig. 2) in a steady state. Although a similar strategy has been employed in RPIS (1979) and DAEWOO *et al.* (1999), some points observed there are revised and refined in the proposed method. First, equilibrium should be set for heat flow rates rather than the heat fluxes. Heat flow rate is obtained by multiplying the heat flux by the relevant area. Therefore, a thermal equilibrium equation can be set up for heat fluxes only when the area through which the heat passes does not change. Second, the effect of convection between the outer face and the environment should be considered, in which the outer face temperature makes a slight difference from the ambient temperature. Many conventional designs neglect this effect. But this oversight is difficult to justify in the LNG tank, especially since the temperature gradient is rather steep under the LNG leakage condition.

To efficiently introduce the convection effect into the present formulation, a concept of equivalent convection thickness is devised. This indicates an additional imaginary thickness of concrete attached to the actual concrete thickness by which we can conveniently set the surface temperature equal to the ambient temperature. Convection heat flux can be expressed by Eq. (1), where ΔT is a temperature difference between the surface and environment, and h_c is the convection coefficient of the concrete. Heat flux by conduction in a surface normal direction (n) through the imaginary concrete thickness ($t_{c,eq}$) is expressed in Eq. (2), where λ_c is the thermal conductivity of the concrete. By equating Eqs. (1) and (2), an equivalent convection thickness can be calculated, as in Eq. (3).

$$q = h_c \Delta T \quad (1)$$

$$q = \lambda_c \frac{\partial T}{\partial n} = \lambda_c \frac{\Delta T}{t_{c,eq}} \quad (2)$$

$$t_{c,eq} = \frac{\lambda_c}{h_c} \quad (3)$$

In Fig. 2, three kinds of heat flow rates are considered— Q_0 and Q_2 for the heat conduction and Q_1 for the heat radiation, as follows:

$$Q_o = \left(\lambda_c \frac{T_a - T_b}{t_c} \right) A_{roof} \quad (4)$$

$$Q_1 = \{F\varepsilon\sigma[(T_b + 273)^4 - (T_c + 273)^4]\} A_{roof} \tag{5}$$

$$Q_2 = \left(\lambda_d \frac{T_c - T_d}{t_d}\right) A_{deck} \tag{6}$$

where λ_d is the thermal conductivity of the deck insulation; t_c and t_d are the thicknesses of concrete roof and deck insulation, respectively; A_{roof} and A_{deck} are the areas of the roof and suspended deck, respectively; F is the form factor; ε is the emissivity; and σ is the Stefan-Boltzmann constant. Here, the conduction effects of the carbon steel liner attached inside the concrete roof and the suspended deck itself may be neglected due to their negligible thicknesses and high thermal conductivities. Note that t_c should be calculated by adding the equivalent convection thickness to the outer face of the actual concrete thickness. The resultant emissivity in Eq. (5) can be calculated taking into account an interaction of two relevant materials as shown in Eq. (7):

$$\varepsilon = \frac{1}{\frac{1}{\varepsilon_{cs}} + \frac{1}{\varepsilon_d} - 1} \tag{7}$$

where ε_{cs} is the emissivity of the carbon steel liner and ε_d that of the deck insulation. When a heat balance is achieved in an equilibrium condition, the equality of Eqs. (4) to (6) can be established. We can determine the temperatures shown in Fig. 2 by solving these nonlinear systems of equations as represented in Eq. (8).

$$Q_0 = Q_1 = Q_2 \tag{8}$$

3.2 Alternative 2

Alternative 2 theorizes a slightly different equilibrium state from that in alternative 1 (Fig. 3). It considers two kinds of heat flow rates, Q_0 and Q_2 , related to heat conduction and inner space temperature, T_e . The form of Q_0 is similar to that in Eq. (4), but T_e is used instead of T_b , and t_c includes the equivalent convection thicknesses in both the outer and inner faces. Similarly, Q_2 resembles Eq. (6), but T_e replaces T_c . Heat balance brings the two heat flow rates into an equilibrium condition, by which we can obtain T_e . Finally, the inner face temperature of the roof can be predicted from T_e .

4. Boundary conditions of wall and bottom slab

To reasonably predict the inner face temperatures of the wall or bottom slab while taking into consideration the effect of insulation layers (Fig. 4(a)), two alternatives are presented. Alternative 1

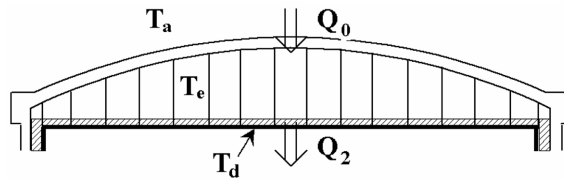


Fig. 3 Heat flow rates through the roof (alternative 2)

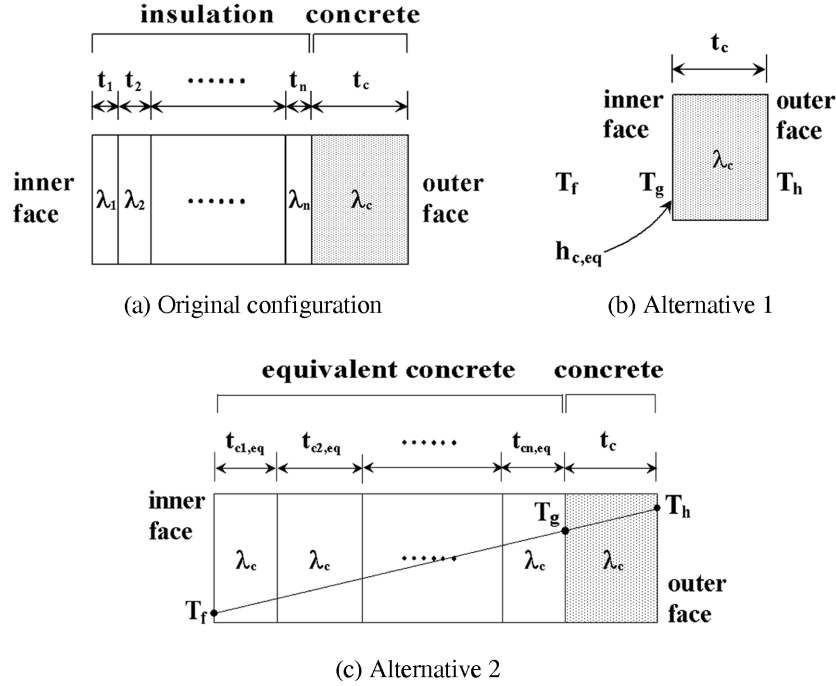


Fig. 4 Analysis schemes of the wall and bottom slab

is the proposed method and alternative 2 employs a conventional scheme with some modifications. Both schemes consider the equivalent convection thickness of Eq. (3) for the outer face of the wall. In the following sections, these two alternatives are compared and the validity of the adopted schemes is discussed in detail.

4.1 Alternative 1

In alternative 1, the effect of each insulation denoted by subscript i is converted into an equivalent convection coefficient ($h_{ci,eq}$) by expressing the actual heat conduction through the insulation (on the left side of Eq. (9)) as the equivalent heat convection (on the right side of Eq. (9)):

$$q = \lambda_i \frac{\Delta T_i}{t_i} = h_{ci,eq} \Delta T_i \tag{9}$$

where λ_i and t_i are the thermal conductivity and thickness of an i th insulation. Since the total n insulation layers are arranged in a series, the resultant equivalent convection coefficient ($h_{c,eq}$), which should be applied to the inner face of the concrete as shown in Fig. 4(b), can be obtained by Eq. (10). This comes from a fact that total resistance of the composite materials combined in a series can be obtained by summing up the resistance of each material and in a convection problem the resistance corresponds to an inverse of the convection coefficient.

$$\frac{1}{h_{c,eq}} = \sum_{i=1}^n \frac{1}{h_{ci,eq}} = \sum_{i=1}^n \frac{t_i}{\lambda_i} \tag{10}$$

4.2 Alternative 2

Alternative 2 converts insulation into equivalent concrete with the condition that the heat flux should be equivalent even after the conversion, as shown in Eq. (11) and Fig. 4(c), by which the equivalent concrete thickness ($t_{ci,eq}$) corresponding to an i th insulation can be obtained in Eq. (12).

$$q = \lambda_i \frac{\Delta T_i}{t_i} = \lambda_c \frac{\Delta T_i}{t_{ci,eq}} \quad (11)$$

$$t_{ci,eq} = \frac{\lambda_c}{\lambda_i} t_i \quad (12)$$

It is clear from the form of the one-dimensional heat conduction equation that the temperature gradient is linear through all the thicknesses, including through the equivalent concrete thicknesses under the steady state. As a result, the inner face temperature (T_g) can be derived as in Eq. (13).

$$T_g = T_h - \frac{T_h - T_f}{\left(\sum_{i=1}^n t_{ci,eq} \right) + t_c} \times t_c \quad (13)$$

4.3 Discussion

Alternative 2 has been widely employed to predict temperature distribution by simple hand calculations (DAEWOO *et al.* 1999). However, the base theory and the validity of the calculation have not been thoroughly examined. The aforementioned procedures are based on heat conduction theory for a one-dimensional case. Therefore, the theories can be applied to the bottom slab precisely but can be approximately applied to the wall. Strictly speaking, the temperature distribution of the wall part of circular tank structures follows the axisymmetric heat conduction theory shown in Eq. (14):

$$Q = \lambda \frac{\Delta T}{\log_e \left(\frac{r+t}{r} \right)} \times 2\pi L \quad (14)$$

where the heat flow rate (Q) is represented for the circumference of a circular wall and the wall height (L). Referring to Fig. 5, when the Eq. (14) is employed instead of the one-dimensional theory, the equality of the Eq. (9) (alternative 1) is modified to the Eq. (15) by which the equivalent convection coefficient is produced in Eq. (16). Equivalent concrete thickness in alternative 2 (Eq. (12)) can also be more accurately determined following Eqs. (17) and (18). Here, $r_{ci,eq}$ indicates a new radius of r_i when the corresponding insulation is converted to the equivalent concrete.

$$Q = \lambda_i \frac{\Delta T_i}{\log_e \left(\frac{r_i + t_i}{r_i} \right)} \cdot 2\pi L = h_{ci,eq} \Delta T_i \cdot 2\pi \left(r_i + \frac{t_i}{2} \right) L \quad (15)$$

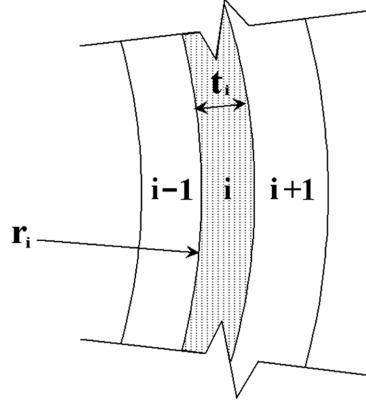


Fig. 5 Insulation layers

$$h_{ci,eq} = \frac{\lambda_i}{\left(r_i + \frac{t_i}{2}\right) \log_e \left(\frac{r_i + t_i}{r_i}\right)} \quad (16)$$

$$Q = \lambda_i \frac{\Delta T_i}{\log_e \left(\frac{r_i + t_i}{r_i}\right)} \cdot 2\pi L = \lambda_c \frac{\Delta T_i}{\log_e \left(\frac{r_i + t_i}{r_{ci,eq}}\right)} \cdot 2\pi L \quad (17)$$

$$r_{ci,eq} = (r_i + t_i) \left(\frac{r_i}{r_i + t_i}\right)^{\lambda_c/\lambda_i} \quad \text{and} \quad t_{ci,eq} = r_i + t_i - r_{ci,eq} \quad (18)$$

For a heat transfer problem of the objects with small radius, e.g., pipes, the exact logarithmic form of Eq. (14) should be employed. Observing the form of the Eq. (14), it can be noticed that the temperature gradient becomes less steep along the wall thickness when proceeding from the inside to the outside. The reason why a one-dimensional theory can be alternatively applied to the heat transfer through the LNG tank wall is that, for almost all the LNG tank dimensions, the radius (r) is sufficiently larger than the thickness (t) of the concrete wall or the wall insulation layers. For such conditions, it can be proven that axisymmetric theory is well approximated to a sufficient degree of accuracy using one-dimensional theory. By substituting the Taylor series expansion of the natural logarithm of Eq. (19) into Eq. (14), the one-dimensional heat conduction equation of Eq. (20) can be derived, where $2\pi rL$ indicates nothing but the area. It also indicates that the logarithmic temperature distribution of Eq. (14) can be approximated by the linear distribution of Eq. (20). In other words, the change of the temperature slope is almost zero for a sufficiently large radius. Take, for example, an insulation layer of an LNG tank, $r_i = 45.95$ m, $t_i = 0.05$ m, $\lambda_i = 0.023$ W/(m \cdot °C), $\lambda_c = 2.324$ W/(m \cdot °C). In this case, Eq. (9) yields $h_{ci,eq} = 0.46$ W/(m 2 ·°C) and Eq. (16) also results in a very similar value. Also, Eq. (12) yields $t_{ci,eq} = 5.052$ m while Eq. (18) results in 4.787 m. It can be identified that the difference of the results of two theories is almost negligible or within an acceptable range of error. Additional comparisons for some other typical LNG tank dimensions and insulations show the similar aspect. The validity of this approximation will be further discussed through numerical examples.

$$\log_e\left(\frac{r+t}{r}\right) = \log_e\left(1 + \frac{t}{r}\right) = \frac{t}{r} - \frac{1}{2}\left(\frac{t}{r}\right)^2 + \frac{1}{3}\left(\frac{t}{r}\right)^3 - \dots \approx \frac{t}{r} \quad (19)$$

$$Q = \lambda \frac{\Delta T}{t} \times 2\pi r L \quad (20)$$

ACI 349R-01 (2001) that is a widely used design code with regard to the nuclear safety related concrete structures also suggests using equivalent linear temperature distribution instead of nonlinear distribution in the containment wall, though from a point of view differing from that of the present discussion. It will be further discussed in a later section.

Though it would appear that alternatives 1 and 2 employ rather different approaches, it can be demonstrated by the following derivations that the final results of the temperature boundary conditions of the wall or bottom slab are essentially the same. In alternative 1, under the steady state the convection condition of the concrete inner face can be converted into the fixed temperature condition by the equality of heat fluxes produced from the convection of the inner face and conduction (Eq. (21)). Rearranging Eq. (21), the inner face temperature is produced, as shown in Eq. (22). Substituting Eqs. (10) and (12) for Eq. (13) and rearranging, the identical result to Eq. (22) is produced, by which the equality of the two alternatives is proved.

$$h_{c,eq}(T_g - T_f) = \lambda_c \frac{T_h - T_g}{t_c} \quad (21)$$

$$T_g = \left(\frac{h_{c,eq}t_c}{h_{c,eq}t_c + \lambda_c}\right)T_f + \left(\frac{\lambda_c}{h_{c,eq}t_c + \lambda_c}\right)T_h \quad (22)$$

Finally, as shown in the above derivations, the inner face boundary condition of an LNG tank can be expressed either by fixed temperature or by convection, and both produce essentially the same results for the general parts. One disadvantage of using the fixed temperature condition, however, is that it cannot elegantly represent a transition zone of temperature near a joint of two fixed temperatures, such as at the joint of the roof and the wall or the wall and the bottom slab, whereas a convection condition naturally forms the transition zone. To improve this problem, the derived fixed temperature can be converted into the convection boundary condition. By adopting Eq. (21) again, but with $h_{c,eq}$ replaced by h_c , Eq. (23) can be derived, indicating that the convection condition with the convection coefficient h_c can be employed along with the equivalent ambient temperature T_f instead of the fixed temperature T_g (refer to Eq. (3) for $t_{c,eq}$). The same concept can be applied to the roof.

$$T_f = T_g + \frac{\lambda_c}{h_c t_c}(T_g - T_h) = T_g + \frac{t_{c,eq}}{t_c}(T_g - T_h) \quad (23)$$

5. Material properties under cryogenic condition

5.1 Concrete

According to previous experiments (Goto and Miura 1979, Ivanyi 1987, Miura 1989), concrete

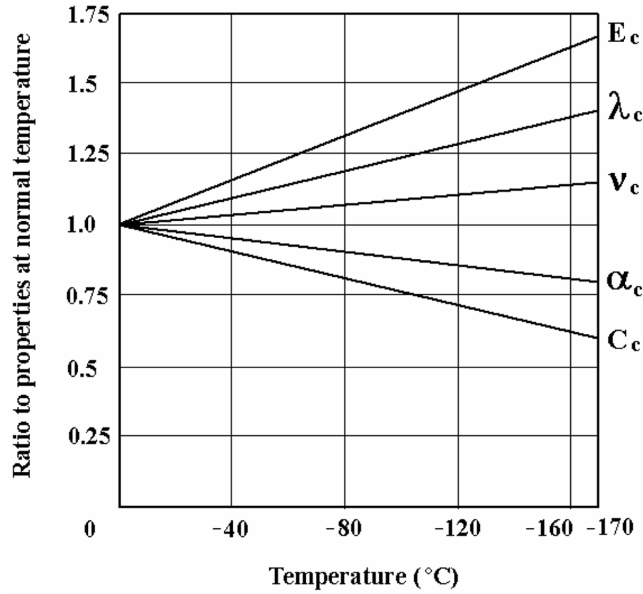


Fig. 6 Change of concrete properties under the cryogenic temperature

undergoes remarkable changes when subjected to cryogenic temperatures and therefore proper consideration of this change is a key to getting realistic thermal analysis results. Nevertheless, such a change of material properties has often been ignored, or only partially considered, or even incorrectly taken into account in many studies or designs. In this study, change of the concrete properties under the cryogenic temperature is strictly considered referring to the available data.

Thermal conductivity linearly increases by about 40% up to -170°C starting from the value at 0°C , while specific heat linearly decreases by about 40% for the same condition (Ivanyi 1987). Coefficient of thermal expansion linearly decreases by about 20% under the same cryogenic condition (Bangash 1989). Reliable experimental data on the convection coefficient under cryogenic condition is not yet available, so the value at normal temperature is applied. The temperature-dependent change of Poisson's ratio shows a wide variation, but on average a 15% increase is assumed up to -170°C .

As the temperature drops below the freezing point, pore water inside the concrete freezes and the volume of water increases. This phenomenon makes the internal structure of the concrete denser, which results in an increase of strength and modulus of elasticity (Goto and Miura 1979, Miura 1989). According to the experiments, the increases of the compressive and tensile strengths follow the Eqs. (24) and (25). In these equations expressed as a unit of kgf/cm^2 , f_{ck} and f_t are the compressive and tensile strengths, respectively, and Δ indicates the increment. w is the water content assumed as 5% in this study. The modulus of elasticity increases linearly by approximately 75% up to -190°C from the value at 0°C . Fig. 6 shows the change of various properties under the cryogenic temperature with the notations referred to the numerical example.

$$\Delta f_{ck} = \left[120 - \frac{1}{270}(T + 180)^2 \right] w \quad T > -120^{\circ}\text{C} \quad (24a)$$

$$\Delta f_{ck} = 107w \quad T < -120^\circ\text{C} \quad (24b)$$

$$f_t = 0.38f_{ck}^{3/4} \quad T > -160^\circ\text{C} \quad (25a)$$

$$\Delta f_t = 6.4w \quad T < -160^\circ\text{C} \quad (25b)$$

5.2 Insulations

A variety of insulations used for the LNG tank also have the temperature-dependent properties to some extent. According to the available data (VDI 2003), it was reported that the thermal conductivities of those insulations decrease as the temperature drops as low as the LNG temperature showing an opposite tendency to that of the concrete. Judging from the Eq. (12), as the thermal conductivity of the insulation decreases, the equivalent concrete thickness increases, which means that the temperature of the actual concrete wall or bottom slab can be maintained relatively high comparing with the results of the proposed methods in section 4. However, the exact calculations considering the change of the insulation properties are not easy to be arranged in a closed form such as Eqs. (13) or (22) because the temperature distribution through the insulations and the concrete is interrelated with the temperature-dependent properties. It indicates that the iterative procedure may be required. From a practical and conservative point of view, it is recommended that the change of thermal conductivity of the insulation be neglected so as to produce lower temperature and steeper gradient in the concrete sections.

6. Calculation procedure of section forces from the nonlinear thermal stress

6.1 ACI 349 procedure

In the ACI 349 procedure (2001), it is recommended that the section forces induced by an actually nonlinear temperature distribution (T_{NL}) are determined from the equivalent linear temperature distribution (T_L). The linear temperature line is so determined as to produce the same temperature-induced moment as that in the nonlinear case. Referring to Fig. 7, an average temperature (T_m) and a gradient (ΔT) can be determined by Eqs. (26) and (27).

$$T_m = (1/h) \int_{-h/2}^{h/2} (T_{NL} - T_b) dy \quad (26)$$

$$\Delta T = (12/h^2) \int_{-h/2}^{h/2} T_{NL} y dy \quad (27)$$

Although it is a simple method oriented for practical engineers, it is inevitable to lose some accuracy from the linear approximation especially for the LNG leakage case that causes more nonlinearity in the temperature distribution. Also, the errors of the stresses may be magnified since the approximation is applied to the temperature, not to the stress itself. Therefore, a more accurate procedure is required to evaluate the stresses caused by the cryogenic LNG as will be proposed in the following.

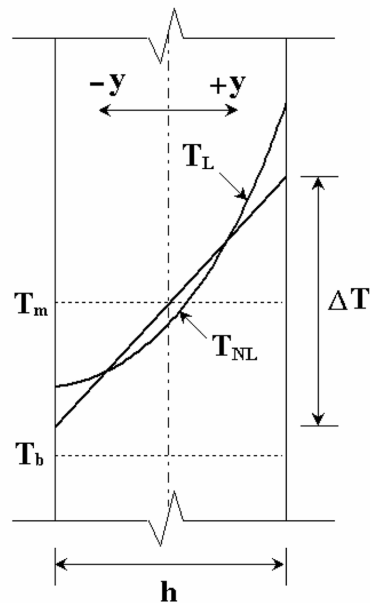


Fig. 7 Equivalent linear temperature distribution by ACI 349

6.2 Proposed procedure

When the finite element method is employed as a thermal analysis tool, a proper element type should be selected according to the shape of the structure under consideration and the purpose of the analysis. For instance, axisymmetric solid elements have been frequently employed in the thermal analysis of LNG tank under normal operation and leakage conditions. In the usual design process, combinations of section forces produced from a variety of load cases should be calculated to check the safety or serviceability of the sections. However, when employing solid elements in the thermal analysis as in this study, the primary output is the stresses, not the section forces; thus, a proper conversion procedure is required to obtain the corresponding section forces used for the load combinations.

When the linear stress distribution is produced from general loads, such section forces as the bending moment and axial force can be obtained in a rather straightforward way from the linear stress. However, temperature-induced stresses in circular storage tanks often exhibit nonlinear distribution through the concrete thickness, resulting from the nonlinear temperature distribution and the internal restraint effect, etc. (Ivanyi 1987, Ghali and Elliott 1992). This nonlinear trend is accelerated when the one face of the wall is subjected to a severe temperature rise or drop, e.g., fire or cryogenic LNG respectively. Moreover, there are some more factors that make the temperature nonlinear for the case in concern: an intrinsic logarithmic distribution of the temperature for a wall of the circular storage tank that has been discussed in section 4.3; and difference of the thermal properties through the concrete thickness depending on a different temperature.

Fig. 8(a) represents a typical example of the temperature-induced nonlinear stress. The proposed method is based on the idea that the nonlinear distribution can be expressed as a sum of the three parts shown in Fig. 8(b), where the constant stress contributes to the axial force and the linear stress

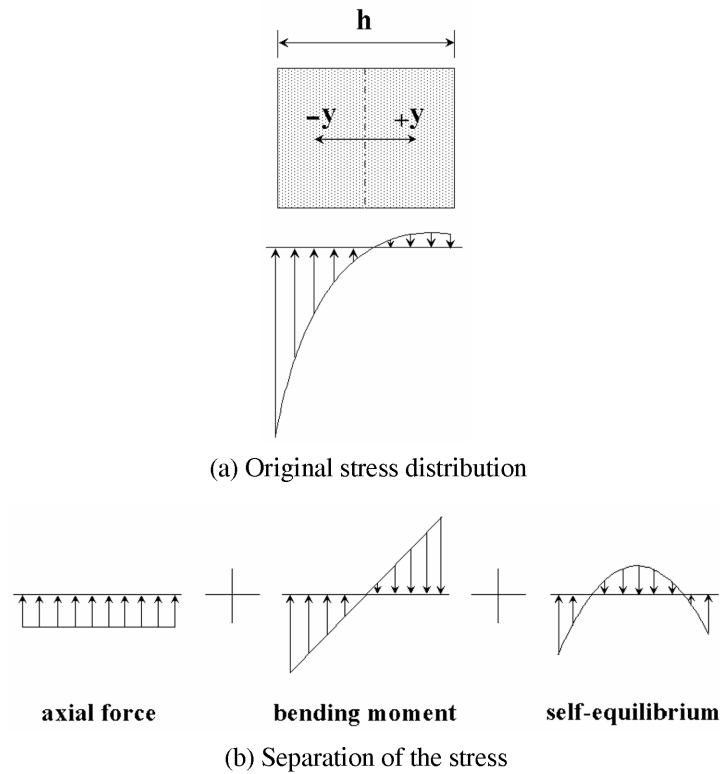


Fig. 8 Separation of thermal stress

to the bending moment. On the contrary, the remaining nonlinear stress results in a self-equilibrium state and does not contribute to the section force, as it is equilibrated by itself (Ghali and Favre 1994). A simple yet useful procedure to separate a rather complex stress distribution into the corresponding section forces is proposed. This procedure does not rely on the linear approximation of the nonlinear temperature distribution, as does ACI 349R-01 (2001), and thus can produce exact section forces based on the actual temperature distribution and stress state. It can be applied to any type of structure that possibly has the nonlinear stress distribution through the section. The proposed procedure is summarized as follows.

- (1) Express the nonlinear stress distribution by Eq. (28) and interpolate the nodal stresses to determine the unknown coefficients a and b and the form of $f(y)$. Here, y is a distance from the center of the section.

$$\sigma = f(y) + ay + b \tag{28}$$

- (2) Assume a distribution of the self-equilibrated stress as the form of Eq. (29).

$$\sigma_{se} = f(y) + a_1y + b_1 \tag{29}$$

- (3) Since the self-equilibrated stress does not produce any section forces such as the axial force and bending moment, Eq. (30) can be established. This can be expressed in explicit forms with respect to the unknown coefficients a_1 and b_1 in Eq. (31). Here, A is area and h height of the section.

$$\int \sigma_{se} dA = 0 \quad \text{and} \quad \int \sigma_{se} y dA = 0 \quad (30)$$

$$a_1 = -\frac{12}{h^3} \int_{-h/2}^{h/2} f(y) y dy \quad \text{and} \quad b_1 = -\frac{1}{h} \int_{-h/2}^{h/2} f(y) dy \quad (31)$$

- (4) The stress distribution that is related to the section forces can be found by $\sigma - \sigma_{se}$. Then, the linear stress $\sigma_m = (a - a_1)y$ contributes to the bending moment in Eq. (32), where I is a moment of inertia of the section. The constant stress $\sigma_n = b - b_1$ contributes to the axial force in Eq. (33).

$$M_t = \frac{\sigma_m I}{y} = (a - a_1) I \quad (32)$$

$$N_t = \sigma_n A = (b - b_1) A \quad (33)$$

7. Application to the assessment of liquid tightness

The proposed consistent thermal analysis procedure has a wide range of applications. Besides leading to a more reasonable design of the sections, it can be usefully adopted in a liquid tightness design of LNG tank incorporating cryogenic temperature-induced stresses (Shekarchi *et al.* 2002, Jeon 2004, Jeon *et al.* 2004). Normally the inner tank contains LNG (Fig. 1), but when the LNG leaks from the inner tank the outer concrete tank comes into contact with LNG. Under this accidental case, it is indispensable for the outer tank to keep the liquid tightness in order to safely contain the LNG before taking any countermeasure. The cryogenic temperature-induced stresses may seriously deteriorate the liquid tightness property of the concrete.

With regard to the liquid tightness design of liquid storage tanks, various code-related specifications exist. The conditions commonly referred in the specifications can be classified into three categories: magnitude of the residual compressive stress; depth of the residual compression zone; and crack width. The importance of each item contributing to the liquid tightness has been appraised differently depending on researchers (Wermann 1998, Rashed *et al.* 2002). In an evaluation of the crack width, it is more recommended to refer to the experimental data of the prestressed concrete members (Nawy 1985, Suri and Dilger 1986) rather than the reinforced concrete members since a wall of the LNG tank is prestressed in most cases using hoop tendons and, if necessary, vertical tendons.

However, note that all three above-mentioned items are closely related to the stresses that can be realistically obtained through the proposed heat transfer analysis and thermal stress analysis procedures. Therefore, the proposed schemes are expected to provide an efficient way of serviceability design of LNG tank that satisfies the various requirements for the liquid tightness.

Table 1 Dimensions of the LNG tank

Sections	Thickness (m)	Remarks
Wall	0.75	General part
Roof	0.6	General part
Bottom slab	1.8	General part
Diameter of wall	92.0	Inner diameter
Radius of curvature of roof	73.6	Inner radius
Height of wall	36.8	Except ring beam
Maximum design liquid level	33.85	

Table 2 Concrete properties at normal temperature

Properties	Value	
	- Outer wall - Ring beam - Bottom slab (annular part)	- Roof - Bottom slab (general part)
Compressive strength (f_{ck}) [N/mm ²]	40	30
Modulus of elasticity (E_c) [N/mm ²]	28000	26000
Poisson's ratio (ν_c)		0.2
Density (ρ) [kgf/m ³]		2300
Thermal conductivity (λ_c) [W/(m·°C)]		2.324
Specific heat (c_c) [J/(kgf·°C)]		920.5
Convection coefficient (h_c) [W/(m ² ·°C)]		12.78
Coefficient of thermal expansion (α_c) [1/°C]		1×10^{-5}

8. Numerical examples

Table 1 shows the thicknesses of the main sections of an LNG tank with 200,000 m³ capacity adopted in this example. Fig. 1 shows the overall shape of the full containment above-ground LNG tank in consideration. Table 2 presents the properties of concrete at normal temperature used in the analyses, and the properties under the cryogenic temperature are considered as previously discussed. The average ambient temperature is set at 35°C assuming the summer and the LNG temperature is conservatively assumed to be -170°C. Heat transfer through the thin plates (inner tank, liner, secondary protection, etc.) can be neglected due to their relative thinness and high thermal conductivities. To perform the heat transfer and thermal stress analyses by the finite element method, a general-purpose structural analysis program ANSYS (2004) is used.

8.1 Heat transfer analysis

8.1.1 Roof

The results of alternatives 1 and 2 are compared here. First, the inner face temperature of the roof is to be calculated according to the alternative 1. A resilient glass blanket is often used as deck

insulation. The form factor (F) (or, alternatively, view factor), which is a function of various factors, is defined with reference to two surfaces that radiate toward each other. However, in the case of a flat dome roof of a typical LNG tank and suspended deck, the form factor can be assumed as a unity. Additionally required information is: $\lambda_d = 0.038 \text{ W/(m}\cdot\text{°C)}$; $t_d = 0.5 \text{ m}$; $\varepsilon_d = 0.96$; $\varepsilon_{cs} = 0.66$; $A_{roof} = 7467.4 \text{ m}^2$; $A_{deck} = 6647.6 \text{ m}^2$; and $\sigma = 5.67 \times 10^{-8} \text{ W/(m}^2\cdot\text{°C}^4)$.

(1) Equivalent convection thickness (Eq. (3)).

$$t_{c,eq} = 2.324/12.78 = 0.182 \text{ m}$$

(2) Emissivity (Eq. (7)).

$$\varepsilon = 1/(1/0.66 + 1/0.96 - 1) = 0.6423$$

(3) Heat flow rates (Eqs. (4) to (6)) with $T_a = 35^\circ\text{C}$ and $T_d = -170^\circ\text{C}$.

$$Q_0 = \left(2.324 \times \frac{35 - T_b}{0.6 + 0.182} \right) \times 7467.4$$

$$Q_1 = \{ 1.0 \times 0.6423 \times 5.67 \times 10^{-8} [(T_b + 273)^4 - (T_c + 273)^4] \} \times 7467.4$$

$$Q_2 = \left(0.038 \times \frac{T_c - (-170)}{0.5} \right) \times 6647.6$$

(4) Solve the nonlinear systems of equations (Eq. (8)).

$$T_b = 30.5^\circ\text{C}$$

Alternative 2, on the other hand, yields the inner face temperature through the following calculations. In this example, the resulting temperature is very similar to that found in the alternative 1.

(1) Heat flow rates with $T_a = 35^\circ\text{C}$ and $T_d = -170^\circ\text{C}$.

$$Q_0 = \left(2.324 \times \frac{35 - T_e}{0.6 + 2 \times 0.182} \right) \times 7467.4$$

$$Q_2 = \left(0.038 \times \frac{T_e - (-170)}{0.5} \right) \times 6647.6$$

(2) Solve the nonlinear systems of equations.

$$T_e = 29.4^\circ\text{C}$$

(3) Calculate the inner face temperature from T_e by applying the modified form of Eq. (23).

$$T_b = 30.5^\circ\text{C}$$

Table 3 Insulation layers of wall

Material	Actual thickness (mm)	Thermal conductivity [W/(m·°C)]	Equivalent concrete thickness (mm)	Remarks
9% Ni inner tank	10		Not considered	
Resilient glass blanket	300	0.038	18347	Lost for leakage
Perlite powder	635	0.040	36894	
PUF	50	0.023	5052	
Carbon steel liner	5		Not considered	
Outer tank wall	750	2.324	750	
Convection effect			182	
Total thickness			Normal operation : 61225 Leakage : 5984	

Table 4 Temperature distribution of wall (Unit: °C)

Location on the wall	Normal operation		Leakage	
	W/ PUF	W/O PUF	W/ PUF	W/O PUF
Inner face	31.9	31.6	3.1	-170
Outer face	34.4	34.3	28.8	-5.0
Atmosphere	35.0	35.0	35.0	35.0

Table 5 Comparison of temperature distribution of wall (Unit: °C)

Location on the wall	Analysis method	Normal operation	Leakage
Inner face	Full model (axisym.; exact)	31.9	3.4
	Full model (1D)	31.9	3.1
	Proposed method	31.9	3.1
Outer face	Full model (axisym.; exact)	34.4	28.9
	Full model (1D)	34.4	28.8
	Proposed method	34.4	28.8

8.1.2 Wall

Since the alternatives 1 and 2 yield the identical results, calculation results of the alternative 2 are only provided in this example. Table 3 shows the thicknesses and thermal conductivities of typical insulation layers and the corresponding equivalent concrete thicknesses. In this system, PUF (Poly-Urethane Foam) is attached to the inner face of the wall and behaves as a cold resistance relief during a leakage accident.

By applying Eq. (13) with $T_h = 35^\circ\text{C}$ and $T_f = -170^\circ\text{C}$, Table 4 is obtained. According to the present procedure, it is relatively convenient to find the effect of LNG leakage on temperature distribution of the outer tank and the effectiveness of cold resistance relief (e.g. PUF). As shown in Table 4, in normal operation PUF does not seriously affect the temperature distribution when

Table 6 Insulation layers of bottom slab

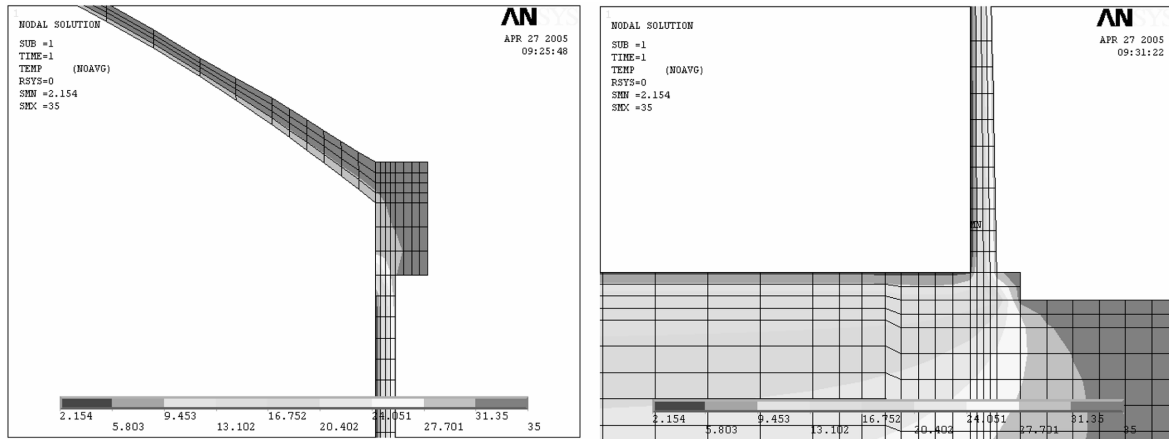
Material	Actual thickness (mm)	Thermal conductivity [W/(m·°C)]	Equivalent concrete thickness (mm)	Remarks
9% Ni inner tank	6		Not considered	
Ply wood	12	0.209	133	
Dry sand	88	1.104	185	Lost for leakage
Foam glass 1	200	0.038	12232	
Dry sand	95	1.104	200	
9% Ni secondary protection	5		Not considered	
Ply wood	12	0.209	133	
Dry sand	88	1.104	185	
Foam glass 2	300	0.048	14525	
Dry sand	95	1.104	200	
Carbon steel liner	5		Not considered	
Outer tank bottom slab (distance to the heater)	900	2.324	900	
Total thickness			Normal operation : 28693 Leakage : 15943	

compared to the non-PUF case, while it does have a pronounced influence on the outer wall in LNG leakage, diminishing the temperature drop and rendering the temperature gradient less steep.

To verify the proposed procedures, the results are compared with the detailed finite element analyses provided by ANSYS, with all the insulation layers included in the finite element modeling (called “full model” in Table 5). The full modeling is conducted in two ways by adopting axisymmetric solid elements and two-dimensional solid (plane) elements to evaluate the accuracy of the proposed scheme. The present procedure produces identical results (see Table 5) to those obtained with a full modeling with the two-dimensional elements. This is expected, as the procedure is based on one-dimensional assumptions. While exact results of the actual axisymmetric situation can be obtained by adopting the axisymmetric elements, Table 5 shows that approximate two-dimensional elements, and thus the proposed method, can predict with sufficient accuracy actual temperatures for LNG tanks of typical dimensions. Of course, if we used the exact logarithmic equation (refer to Eq. (14)), it would produce the identical results to those of the axisymmetric elements.

8.1.3 Bottom slab

The heating system is inserted in a middle of the bottom slab and is maintained at a constant temperature of 15°C in this example following a usual manner. The insulation layers below the secondary protection are preserved even in the leakage (Table 6). Following a procedure similar to that applied for the wall, the inner face temperature is predicted to be 9.2°C for normal operation and 4.6°C for leakage. For the bottom slab, the proposed scheme produces the identical results to those of the finite element analyses.



(a) Joint of roof and wall

(b) Joint of wall and bottom slab including sub-soil

Fig. 9 Temperature distribution of the LNG tank

8.1.4 Discussion

In the proposed scheme, inner face temperatures can be predicted even by the hand calculations, thus eliminating the necessity for complicated full finite element analyses of all the insulation layers and the suspended deck. In previous design documents and researches, the inner face temperature of the wall and bottom slab is unjustifiably assumed to be the LNG temperature for the leakage case. However, it has been shown in this example considering the beneficial effects of preserved insulation that the temperature may be quite above the LNG temperature. The example also predicts, as distinct from current design practice, that the inner face temperature of the roof is well above the LNG temperature due to a thermal barrier effect of the suspended deck. The above-mentioned wrong assumptions regarding the inner face temperature may result in overestimating the temperature drop or temperature gradient, and an over-design of the concrete sections and reinforcing bars may occur.

The subsequent heat transfer analysis is performed by modeling the outer concrete tank with the temperature boundary conditions of the inner faces calculated above. The temperature contour for the leakage case found with finite element analysis using the axisymmetric solid elements (PLANE75) is shown in Fig. 9. Sub-soil part is also considered in order to allow a smooth transition of temperature between the tank and the soil. Soil properties are referred to from the available data.

8.2 Thermal stress analysis

A thermal stress analysis for a tank when it is subjected to the temperature distribution resulting from the preceding heat transfer analysis is performed here using PLANE25 (axisymmetric solid elements for stress analysis). The following procedure shows an application of the proposed method for predicting section forces per unit length from the nonlinear thermal stresses.

- (1) Obtain the stress values at a checking point. For example, in the case of leakage, the hoop stresses at an upper part of the wall are 4.7145, 2.4160, 0.13395, -2.1301, -4.3791 in N/mm² (positive in tension) at five equally spaced nodal points, in an order from the inner face to the outer face.
- (2) When the nodal point values are interpolated by assuming, for example, the Lagrange polynomial, the following equation is obtained (Eq. (28)). Here, positive y is set outward in mm.

$$\sigma = -1.5170 \times 10^{-13} y^4 - 1.7699 \times 10^{-11} y^3 + 2.6133 \times 10^{-7} y^2 - 1.2122 \times 10^{-2} y + 1.3395 \times 10^{-1} \text{ N/mm}^2$$

- (3) Obtain a_1 and b_1 (Eq. (31)).

$$a_1 = 1.4933 \times 10^{-6} \text{ N/mm}^3$$

$$b_1 = -1.1650 \times 10^{-2} \text{ N/mm}^2$$

- (4) Obtain the bending moment and the axial force (Eqs. (32) and (33)).

$$M_t = -4.2623 \times 10^5 \text{ N}\cdot\text{m} \quad (\text{inward convex})$$

$$N_t = 1.0920 \times 10^5 \text{ N} \quad (\text{tension})$$

9. Conclusions

Since the LNG tank should safely contain cryogenic LNG (Liquefied Natural Gas), primary importance should be placed on the thermal analyses in assessing the safety or serviceability of concrete sections of the tank. However, structural details of the LNG tank are so complicated that special attention should be paid in order to perform a reliable analysis.

In this paper, several methodologies were devised for predicting the temperature boundary conditions of inner faces of the outer concrete tank and for setting up a reasonable heat transfer analysis model for a full containment above-ground LNG storage tank. The proposed model concentrated on the outer tank and the beneficial effects of insulation layers and a suspended deck on temperature distribution of the outer tank were formulated separately as the boundary conditions of the outer tank. To this aim, the equilibrium of heat flow rates or heat fluxes in a steady state condition was utilized, where various aspects of heat transfer via conduction, convection and radiation were considered. A variety of situations that may occur during normal operation or an LNG leakage accident can be promptly simulated within the proposed outer tank model only by changing the boundary conditions, thus providing a versatility to designers. The thermal properties of the concrete and insulations under cryogenic temperature conditions were discussed and taken into account if necessary. An improved strategy for evaluating the section forces from nonlinear distribution of the thermal stresses was proposed. Some unjustifiable assumptions common in conventional analyses and designs were pointed out.

The proposed schemes were verified through some numerical examples, where the actual

temperature and stress distributions of the LNG tank as affected by the cryogenic LNG could be realistically predicted. It is expected that a more practical and realistic thermal analysis of the LNG tank is possible using the proposed scheme. In addition, the effects of insulation layers and a suspended deck on temperature distribution can be readily detected by the proposed methods even in a preliminary design stage, which helps to minimize the trial and error involved in a detailed design.

References

- ACI Committee 349 (2001), *Commentary on Code Requirements for Nuclear Safety Related Concrete Structures (ACI 349R-01)*, American Concrete Institute, Mich.
- ANSYS - User's Manual. Ver. 8.0 (2004), ANSYS, Inc.
- Association of German Engineers (VDI) and VDI Society for Chemical and Process Engineering (1993), *VDI Heat Atlas*, VDI-Verlag GmbH, Düsseldorf, Germany.
- Bangash, M.Y.H. (1989), *Concrete and Concrete Structures: Numerical Modelling and Application*, Elsevier Applied Science, NY.
- Chen, Q.S., Wegrzyn, J. and Prasad, V. (2004), "Analysis of temperature and pressure changes in liquefied natural gas (LNG) cryogenic tanks", *Cryogenics*, **44**(10), 701-709.
- Choi, C.K., Lee, T.Y. and Lee, E.J. (2002), "Improved finite element models for the in-ground LNG storage tank", *J. the Korean Society of Civil Engineers*, **22**(5-A), 1175-1182.
- DAELIM Industrial Co., Ltd. and DYWIDAG (1995), *Inchon LNG-receiving Terminal (1st Extension)*.
- DAEWOO Corp., DAELIM Industrial Co., Ltd. and OBAYASHI Corp. (1999), *Tongyoung LNG Terminal Project*.
- Ghali, A. and Elliott, E. (1992), "Serviceability of circular prestressed concrete tanks", *ACI Struct. J.*, **89**(3), 345-355.
- Ghali, A. and Favre, R. (1994), *Concrete Structures: Stresses and Deformations*, 2nd ed., E & FN Spon, London.
- Goto, Y. and Miura, T. (1979), "Experimental studies on properties of concrete cooled to about minus 160 °C", *Technology Reports (Tohoku Univ.)*, **44**(2), 357-385.
- Ivanyi, G. (1987), "Local and global cryogenic attacks", *Proc. of the 1st Int. Conf. on Concrete for Hazard Protection*.
- Japan Gas Association (1979), *Recommended Practice for LNG Inground Storage (RPIS)*.
- Jeon, S.J. (2004), "Consistent assessment for liquid tightness of LNG storage tank subjected to cryogenic temperature-induced forces", *J. the Korean Society of Civil Engineers*, **24**(1-A), 203-210.
- Jeon, S.J., Chung, C.H., Jin, B.M. and Kim, Y.J. (2004), "Liquid tightness design of LNG storage tank incorporating cryogenic temperature-induced stresses", *Proc. of CONSEC'04*, Korea.
- Miura, T. (1989), "The properties of concrete at very low temperatures", *Materials and Structures*, **22**(130), 243-254.
- Nakano, M. (2001), "Technological trend and latest technological development of LNG inground storage tanks", *J. Construction Management and Engineering (Japan Society of Civil Engineers)*, **51**(679), 1-20.
- Nawy, E.G. (1985), "Flexural cracking behavior of pretensioned and post-tensioned beams: The state of the art", *ACI J.*, **82**(6), 890-900.
- Rashed, A., Elwi, A.E. and Rogowsky, D.M. (2002), "Reinforced, partially prestressed concrete water tank walls", *ACI Struct. J.*, **99**(3), 288-298.
- Shekarchi, M., Debicki, G., Granger, L. and Billard, Y. (2002), "Study of leaktightness integrity of containment wall without liner in high performance concrete under accidental conditions – I. Experimentation", *Nucl. Eng. Des.*, **213**(1), 1-9.
- Suri, K.M. and Dilger, W.H. (1986), "Crack width of partially prestressed concrete members", *ACI J.*, **83**(5), 784-797.
- Watanabe, N., Endo, H., Xuehui, A., Nakano, M. and Aoki, H. (2003), "Application of non-linear analysis to

- structural design of a LNG inground tank”, *J. Construction Management and Engineering (Japan Society of Civil Engineers)*, **60**(742), 87-100.
- Wermann, T. (1998), “Cryogenic cube tests - Leakage, temperature, deformation”, <http://www.concrete.ct.tudelft.nl>